

# Fast Densification Process in Manufacturing Carbon/Carbon Using Vegetable Precursors

João Jorge Souza dos Santos<sup>1</sup>, Inacio Regiani<sup>1</sup>

## How to cite:

Santos JJS  <https://orcid.org/0000-0003-1183-5479>

Regiani I  <https://orcid.org/0000-0002-5642-2056>

Santos JJS; Regiani I (2018) Fast Densification Process in Manufacturing Carbon/Carbon Using Vegetable Precursors. J Aersp Technol Manag, 10: e2718. doi: 10.5028/jatm.v10.921

**ABSTRACT:** The carbon/carbon composite manufacturing processes generally use flammable and toxic precursors. In order to make these processes safer, it is interesting to use less toxic and safer precursors to the environment and people. The present study investigates the types of pyrocarbon resulting from composite carbon/carbon densification produced by the technique of Film Boiling Chemical Vapor Infiltration using as carbon precursors: soybean oil, ethanol and hexane, the latter as control. The microstructure produced was analyzed through SEM techniques, PLDM, XRD and Raman. The pyrocarbons observed are Smooth Laminar, Rought Laminar and Regenerative Laminar types. Soybean oil resulted in porous bodies while other precursors resulted in denser bodies. The crystallites made with ethanol and hexane have preferential growth in the c direction, while those made with soybean oil grow preferentially in a direction.

**KEYWORDS:** Carbon-carbon, Composites, Porous materials, Chemical Vapor Infiltration.

## INTRODUCTION

The carbon/carbon composite (C/C), also known as Carbon Fiber Reinforced composite (CFRC), form a class of materials with very particular applications in aerospace areas (Bokros *et al.* 1973), such as aircraft breaks and rocket nozzles. The main features that justify its application are maintenance of mechanical properties at temperatures above 1300 °C, low density, chemical inertia, dimensional stability and low thermal expansion coefficient (Murdie 1993; Savage 1993). Due to its good tribological properties and its very low thrombogenicity, pyrocarbon is also largely used in biomedical materials, such as heart valves (Bourrat *et al.* 2006).

One of the alternative processes for the production of C/C is Film Boiling Chemical Vapor Infiltration (FB-CVI). Houdayer *et al.* published in 1984 the first citation on the process of FB-CVI. Since then, researchers produced C/C by FB-CVI using only petrochemical precursors such as cyclohexane, chlorobenzene, toluene, cyclohexane, and kerosene, among others (Rovillain *et al.* 2001; Delhaès *et al.* 2003; 2005; Wang *et al.* 2007; Vignoles *et al.* 2006). There is just one article that reported using ethanol, a liquid precursor from a vegetable source, to produce C/C applied in isothermal CVI process (Li *et al.* 2010). However, the use of petrochemical precursors in several countries, such as Brazil, requires compliance with specific laws related to work safety. As they are carcinogens, they require additional high wages to the worker, as well as the supply of individual and collective protective equipment, including risk of major accidents due to the high flammability characteristic of the precursor (Brasil 1978). Another important point is the matter of waste disposal of the process that shall be in compliance with the environmental legislation of

<sup>1</sup>.Departamento de Ciência e Tecnologia Aeroespacial – Instituto Tecnológico de Aeronáutica – Divisão de Engenharia Mecânica – São José dos Campos/SP – Brazil.

**Correspondence author:** Inacio Regiani | Departamento de Ciência e Tecnologia Aeroespacial – Instituto Tecnológico de Aeronáutica – Divisão de Engenharia Mecânica | Praça Marechal Eduardo Gomes, 50 | CEP: 12.2028-900 – São José dos Campos/SP – Brazil | Email: inacior@ita.br

Received: Mar. 2, 2017 | Accepted: Jul. 26, 2017

**Section Editor:** Mariana Fraga



each country (Brasil 2010). For these two reasons the attempt to use a vegetable carbon precursor is interesting (Brasil 1978; 2010). What differs our research from the others is the use of low toxicity vegetable precursors, which are safer in parts manufacturing using the FB-CVI process.

This paper presents the result of the C/C composite manufacturing using vegetable precursors such as soybean oil and ethanol in the FB-CVI process. It was evaluated its microstructure and the pyrocarbons produced, then they were compared with the results obtained with hexane. The materials produced were analyzed by scanning electron microscopy techniques (SEM), polarized optical light microscopy (PLOM), X-ray diffraction (XRD) and Raman scattering spectroscopy.

## EXPERIMENTAL

A schematic drawing of the FB-CVI reactor used is shown in Fig. 1. The reactor has a capacity of 3000 cm<sup>3</sup> of reactant, made of stainless steel with copper electrodes insulated by a Teflon top. Connectors with low porosity graphite are fixed at their ends to fasten the preform to be densified. The container with the precursor is connected to a vapor condensation system and to a nitrogen inlet to make an inert atmosphere in the reactor. An electric current source of high amperage was connected to the electrodes. In order to control the temperature, a thermocouple connected to the temperature controller was used in direct contact with the carbon fiber yarn that serves as resistor.

The preforms had dimensions of 50 mm × 20 mm × 20 mm. All of them made of SGL Carbon felt with 96% voids and pierced by carbon fiber yarn with Toray T300 with 24 K filaments. This yarn is the resistor. The FB-CVI process is simple to implement: immerse the preform in the liquid precursor, select the desired temperature and switch on the power supply. The precursor liquid used was ethanol, soybean oil and hexane at densification temperatures of 900 °C, 1000 °C, 1100 °C and 1200 °C.

After densification, the samples were analyzed by XRD techniques, Raman spectroscopy, SEM and PLOM. The PLOM technique measured the extinction angle according to the method described by Bourrat *et al.* (2000) using a 560 nm filter. Raman spectroscopy used a 514 nm wavelength with 4 interactions of 60 s for each interaction. All measures of PLOM and Raman were done at 5 mm from the center of preforms, about half radius of the sample.

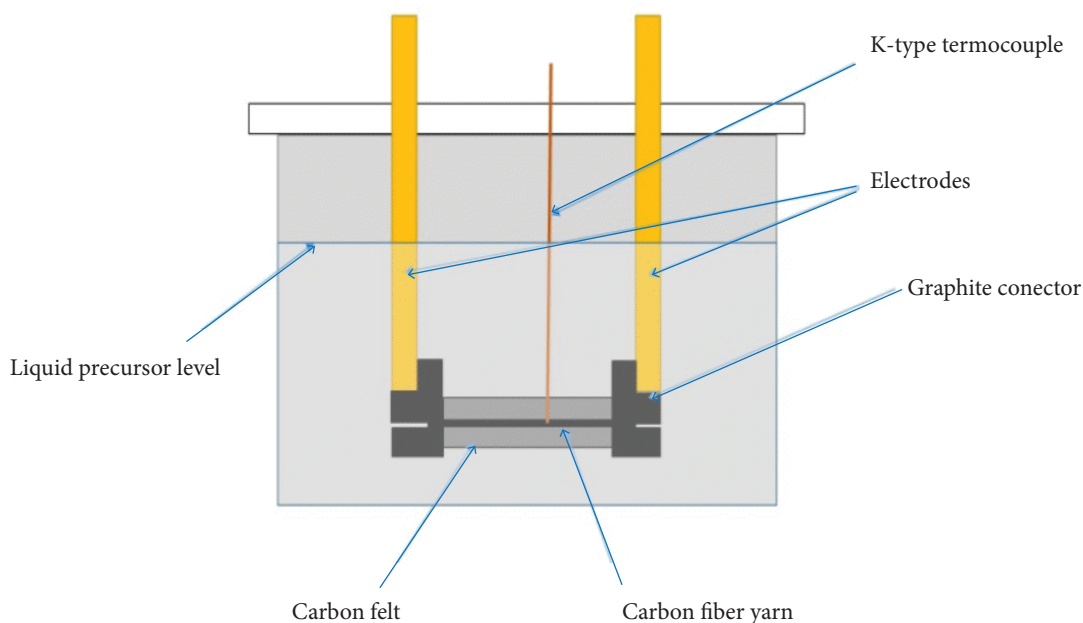


**Figure 1.** Schematic drawing of FB-CVI reactor.

## RESULTS

The XRD spectra shows that the felt is essentially amorphous and the deposited pyrocarbons have some crystallinity, especially the one made with ethanol at 1200 °C, as shown in Fig. 2. The crystallite size in c direction ( $L_c$ ) of the samples was determined using Eq. 1, where  $B$  is the half band width in radians,  $\theta$  is the diffraction angle and  $\lambda$  is the X-ray wave length, in this case 1.5406 Å. The peak chosen was 26° due to its good resolution, other peaks in these XRD are broad and do not refer to a lattice direction. From Table 1 it can be noticed that the crystallite size produced by ethanol at 900 °C, 1000 °C, and 1100 °C is approximately 30 nm, except for the pyrocarbon deposited at 1200 °C. The same is seen in hexane samples which present around 20 nm for temperatures up to 1000 °C and higher than 30 nm at temperatures of at least 1100 °C. In the case of soybean oil, there is a constant size of 27 nm independent on the temperature.

$$L_c = 0.9\lambda/B \cos \theta \quad (1)$$

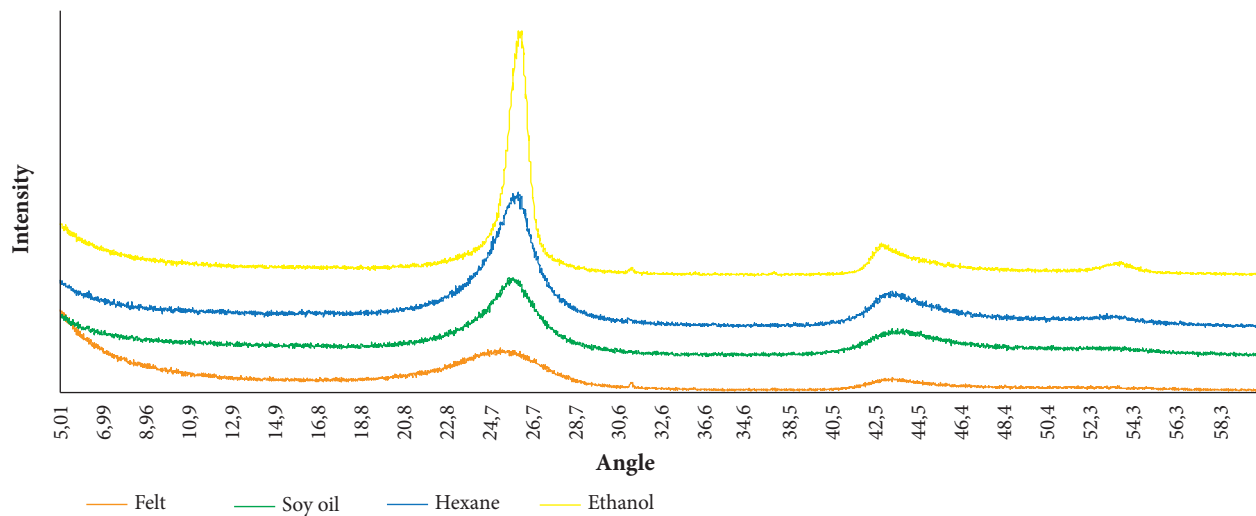


**Figure 2.** XRD of samples made at 1200 °C.

**Table 1.** Crystallite size according to the Scherrer formula in direction c, measured in nanometers (nm).

Precursor	900 °C	1000 °C	1100 °C	1200 °C
Hexane	25.8	22.6	43.5	33.9
Ethanol	36.4	35.9	27.8	80.7
Soybean Oil	27.4	27.4	27.5	27.7

Figure 3 shows the microscopy of the white polarized light of the densified hexane sample at 1200 °C. It is possible to see the optical activity forming the Maltese Crosses in pyrocarbon deposited around the fibers. The optical activity, showed in Fig. 3 and in the measurements of Table 2, results from the existence of crystallinity (Bokros 1965). The extinction angles, whose values are shown in Table 2, were measured using a 560 nm light filter. All values for ethanol and hexane have a variation of 1° above or below, but values for soybean oil have a variation of 5°. The hexane samples showed extinction angle measures between 17° and 19°. All pyrocarbons made with ethanol presented angles of 10° to 11°. Those made with soybean oil presented a large scatter of measurements, from 12° to 21°.

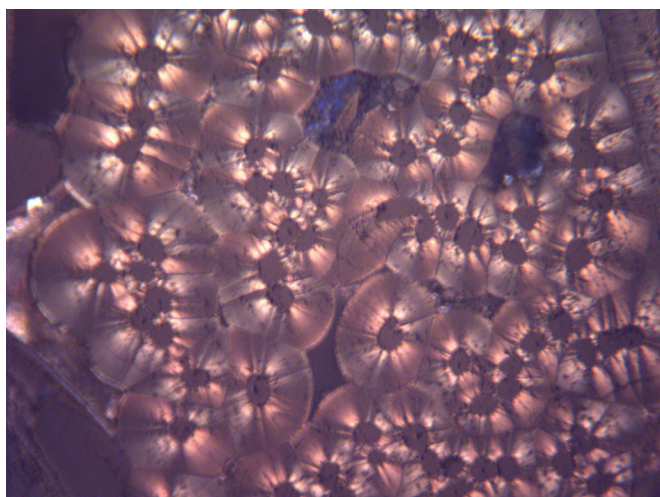


**Figure 3.** Microscopy with white polarized light of hexane samples densified at 1200 °C.

**Table 2.** Measured values of the extinction angle of the samples made with soybean oil, hexane and ethanol densified at 900 °C, 1000 °C, 1100 °C and 1200 °C.

Precursor	900 °C	1000 °C	1100 °C	1200 °C
Hexane	17°	19°	17°	18°
Ethanol	10°	10°	11°	10°
Soybean oil	16°	21°	15°	12°

SEM image shows how the sample structures are densified. Figure 4 shows a well densified section of a sample made with hexane. Figure 5 shows the surface of a fracture from a sample made with ethanol, which is more porous than the hexane one. Yet, Fig. 6 shows how the sample made with soy oil is very porous. In Fig. 7, one can see the front of deposition from which propagation mechanism is the formation of cones growing around the fiber.

Due to a better densification of the samples at 1100 °C, the Raman spectroscopy was performed in these samples (Fig. 8). It shows a significant difference of the carbon that forms the felt, the first below spectroscopy in Fig. 8, with pyrocarbons deposited by the precursors, the other spectroscopies in the same figure.

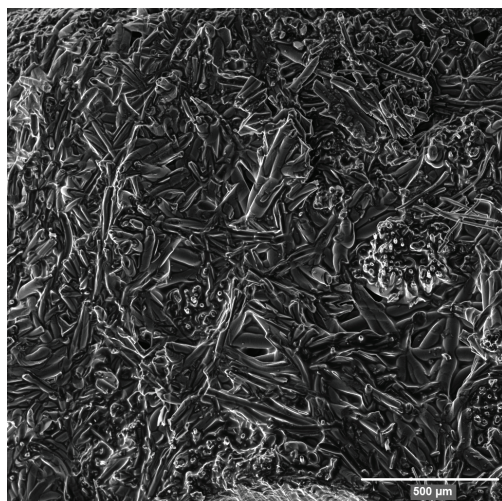


**Figure 4.** SEM image of the fracture of a dense body produced with hexane.

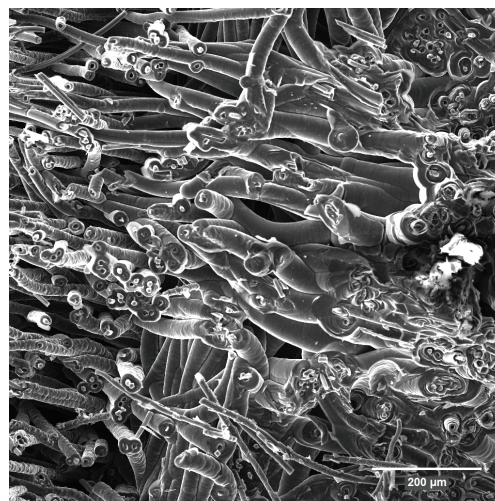


**Figure 5.** SEM image of the fracture of a body produced with ethanol at 1000 °C.

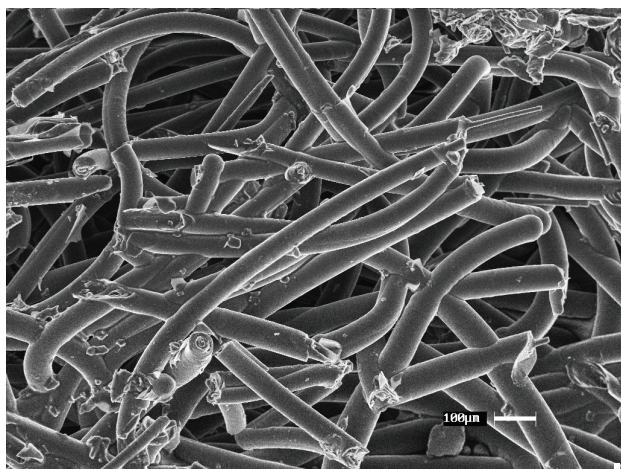


**Figure 6.** SEM image of the interior of a densified sample with soybean oil showing the porosity resulted from the use of this precursor.

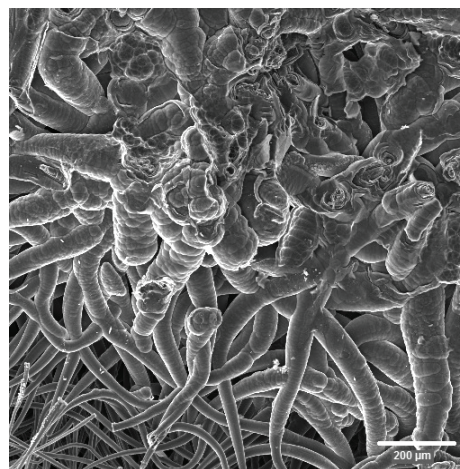


**Figure 7.** SEM image of the cones forming the densification front in hexane precursor.

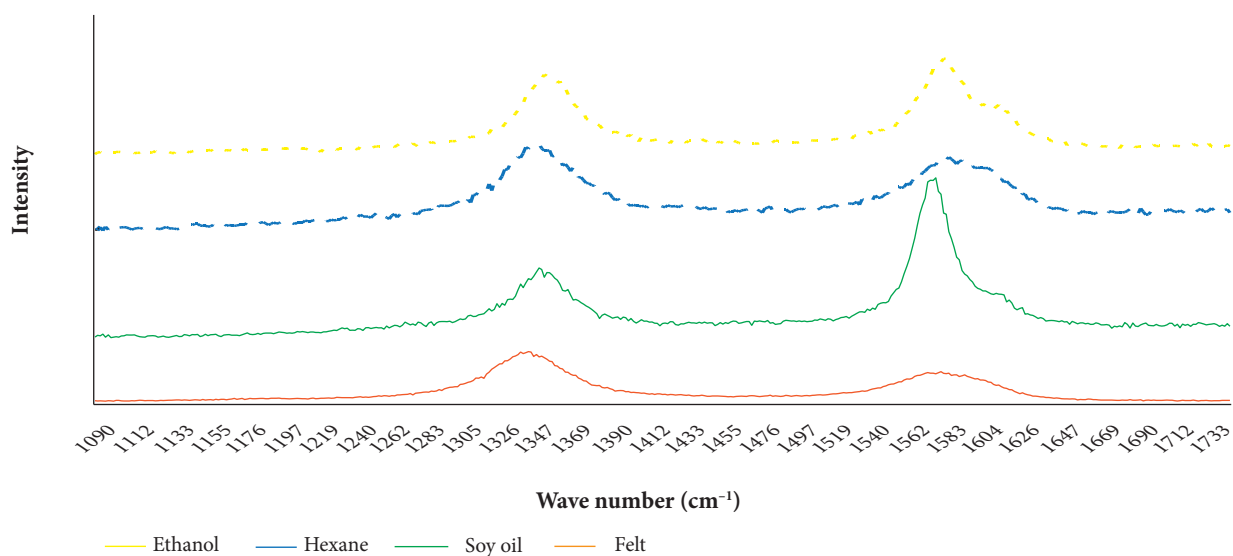


**Figure 8.** Raman spectra from pyrocarbons deposited at 1100 °C and of the felt.

## DISCUSSION

Through XRD and the results of Table 2, it is apparent that despite the increase of the crystallites with temperature, the deposited carbon still presents low crystallinity. This crystallinity can be observed in the presence of optical activity under polarized light in Fig. 3. According to the measurement of the extinction angle, all pyrocarbons deposited by hexane are Rough Lamellar (RL), i.e., they present several crystallites with few defects (Bourrat *et al.* 2006). Ethanol showed larger crystallites at 1200 °C, but smaller for the other temperatures. Ethanol shows a lower angle of extinction, so it can be classified as Smooth Lamellar pyrocarbons type, SL, with the greatest number of defects (Bourrat *et al.* 2006). In contrast, Li *et al.* (2010) produced pyrocarbon with 21 nm of Lc and extinction angle measure from 19° to 21° by I-CVI only after heat-treating the samples at 2500 °C. The soy oil presented extinction angle measurements ranging from the minimum SL threshold, 12°, to the greatest value of 21°, this last measure

indicates the presence of Regenerative Laminar pyrocarbon, ReL (Bourrat *et al.* 2006). The crystallite size formed by soybean oil is constant, as shown in Table 1, being its XRD more amorphous. The small crystallites associated with a great dispersion in extinction angle measures indicate that the soy oil has the capability of depositing different types of pyrocarbon simultaneously on the same specimen; there is SL, RL and ReL pyrocarbons in a small area, as a mosaic of pyrocarbons. This shows that the precursors of lower carbon chain produce a more uniform pyrocarbon; ethanol with more defects and hexane with less defects. However, soybean oil, which has a much longer chain, does not have a defined pyrocarbon.

Figures 3 and 4 show well densified sample sections made in hexane at 1200 °C. These samples reach densities, by Archimedes method, exceeding 1.75 g/cm<sup>3</sup>. Figure 5 shows that the samples are made more porous with ethanol, and the density measured by Archimedes method is 1.60 g/cm<sup>3</sup>. In the case of soybean oil, the density measured by Archimedes method is very low, in the range of 1.35 g/cm<sup>3</sup>. Moreover, the bulk density is sometimes less than 1.0 g/cm<sup>3</sup>, indicating that the sample is porous. Figure 6 shows the high porosity characteristic of parts made with soybean oil, and may classify them as stiff felt.

In one of their publications, Vignoles *et al.* (2005) state that several researchers, both in simulations and practical experiments, observed a mass density variation in the radial direction of the sample, being more porous inside. This is attributed to an imbalance between the volumetric heating and radiation loss (Vignoles *et al.* 2005). Vignoles *et al.* model (Vignoles *et al.* 2006; 2007; Nadeau *et al.* 2006) only provides the results for gas phase, where the viscosity of the precursor was considered irrelevant if compared with liquids ones. In the case of FB-CVI process with soybean oil, the process seems to change, first the oil viscosity is much higher than the light aliphatic hydrocarbons, and the chemical reaction is also very different. Thus, in FB-CVI with soybean oil, the mass transfer may change. As the gas resulting from pyrolysis shall leave the felt preform, the viscosity of the liquid becomes important. In the case of low viscosity liquids, like ethanol and hexane, pyrolysis gas expands easily in and out of the preform, while a new quantity of low viscosity fluid enters the porous preform at a relatively high mass rate. However, when the fluid is viscous, such as soybean oil, the gas expansion and outlet are hampered due to the higher oil viscosity, promoting a kind of sealing. This same viscosity makes it difficult for a new amount of oil to enter the preform, so the inlet mass rate is reduced. The material that produces this sealing is then consumed only thickening the fibers, because the oil vapor residence time inside the felt is greater when compared with the hexane vapor. Thus, the carbon of the oil mist is completely consumed without replenishment of an enough quantity of the new precursor, so the resulting part is porous.

Figure 7 shows the densification front of a sample made with hexane at 1100 °C. It is possible to notice in it that the deposition of pyrocarbon occurs around the felt fibers, thickening them and thus closing the gaps between the fibers. The growth along the fiber occurs because it is conductive of heat, but the temperature on the fiber surface diminishes due to the distance from the already densified region. Thus, there is a thickening of the fibers toward the center of the sample. This micrograph shows that the movement of the densification front is supported by the fibers that form the preform. This conclusion is supported by the graphic, which shows the thickness of deposit in functions of radial distance presented by Rovillain *et al.* (2001). The densification front is not a continuous and dense growth as a CVD film, i.e., the front surface is not flat and well-defined.

For the characterization by Raman spectra, small chips were taken of the samples made at 1100 °C, which exhibited the highest density of Archimedes. They were not polished as recommended by the article of Ammar and Rouzaud (2012) In the spectrum it can be seen that the peak G, 1580 cm<sup>-1</sup>, has become more intense for the precursors of vegetable origin.

Both the felt and the pyrocarbon made with hexane show peak D, at 1332 cm<sup>-1</sup>, greater than peak G. Peak G appears intensively in all spectra. According to Ammar's *et al.* (2012) work, the D peak observed in carbon-carbon composite is unreliable, especially for the polished samples, thus all the Raman features extracted to be used for the characterization of pyrocarbons are restricted to the peak G data. According to Moslava *et al.* (2012), the crystallite size in the direction La is inversely related to the width of the middle band of the G peak, the FWHM (G), as shown by Eq. 2. Using G and D peaks deconvolution of the spectra shown in Fig. 8, it is possible to calculate La. It shows that the soybean oil presents La of 43 nm, ethanol presents La of 18 nm and the hexane presents La of 24 nm. Because La is related to the size of graphite sheet, one could say that the soybean oil is capable of forming carbon rings, but could not do their stacking, since ethanol and hexane could produce a crystal with small aromatic leaves, but more stacked ones, i.e., with a higher Lc.

$$FWHM(G) = 14 + 430/La \quad (2)$$

Considering the values of XRD crystallite at the temperature of 1100 °C (Table 1) and making the ratio  $L_c/L_a$ , one can have an idea of the crystallite aspect ratio. Notice that larger crystallites are formed by soybean oil and hexane, while ethanol forms very small  $L_a$  and  $L_c$ . The hexane and soybean oil have values of  $L_a$  and  $L_c$  changed, the hexane  $L_c/L_a$  ratio is 1.8 and soybean oil is 0.7. The soybean oil and hexane crystallites may have similar sizes, but the format of both is quite different. Since ethanol ratio  $L_c/L_a$  is 1.6, its format is similar to the hexane crystallite. This indicates that the soy oil promotes a greater increase in direction  $a$ , while hexane and ethanol promote further growth in the direction  $c$ .

---

## CONCLUSION

This paper shows that it is possible to densify C/C using ethanol as a precursor in FB-CVI. The main characteristics and conclusions from this work are:

- Ethanol, precursor with small carbon chain, densifies pyrocarbons of the SL type, while hexane densifies preferably RL type pyrocarbon. Yet, soybean oil, which has a large carbon chain, presents various types of pyrocarbon simultaneously as in a mosaic fashion.
- The  $L_c$  crystallite size shows no correlation with the precursor used, but it increases as the temperature increases.
- The parts that had better density and lower porosity in their structure were made with hexane. Soybean oil only thickened the fibers and produced stiff felts. The ethanol was presented as a precursor that resulted in intermediate characteristics. The highest density for all precursors was observed at 1100 °C.
- The densification front is formed by cones from which axis is the fiber in which the Pyrocarbon is deposited.
- Through XRD and Raman spectra, it can be seen that the crystallites made with hexane and ethanol have a higher growth in  $c$  direction, while soybean oil promotes a greater growth in a direction.

---

## AUTHOR'S CONTRIBUTION

Both authors contributed equally to the paper.

---

## ACKNOWLEDGMENTS

This work has been sponsored by FAPESP. Special acknowledge to Prof. Evaldo J. Corat from INPE due to RAMAN spectroscopy.

---

## REFERENCES

- Ammar MR, Rouzaud J-N (2012) How to obtain a reliable structural characterization of polished graphitized carbons by Raman microspectroscopy. *Journal of Raman Spectroscopy* 43(2):207-211. doi: 10.1002/jrs.3014
- Bokros JC (1965) Variation in the crystallinity of carbons deposited in fluidized beds. *Carbon* 3(2):201-211. doi: 10.1016/0008-6223(65)90049-7
- Bokros JC, Lagrange LD, Shoen FJ (1973) Control of structure of carbon for use in bioengineering. In: Walker Junior PI, Thrower PA. In: *Chemistry and Physics of Carbon*. v 9. New York: Marcel Dekker. p. 103-164.
- Bourrat X, Langlais F, Chollon G, Vignoles GL (2006) Low temperature pyrocarbons: a review. *J Braz Chem Soc* 17(6):1090-1095. doi: 10.1590/S0103-50532006000600005
- Bourrat X, Trouvat B, Limousin G, Vignoles GL, Doux F (2000) Pyrocarbon anisotropy as measured by electron diffraction and polarized

light. *Journal of Materials Research* 15(1):92-101. doi: 10.1557/JMR.2000.0017

Brasil (1978) Portaria n. 3.214 de 08 de junho de 1978. Aprova as Normas Regulamentadoras do Ministério de Estado do Trabalho, com redação dada pela Lei nº 6.514 de 22 de dezembro de 1977; [accessed 2018 May 7]. [http://acesso.mte.gov.br/data/files/FF8080B14FF112E801529E4EFC2C655F/Portaria%20n.%C2%BA%203.214%20\(aprova%20as%20NRs\).pdf](http://acesso.mte.gov.br/data/files/FF8080B14FF112E801529E4EFC2C655F/Portaria%20n.%C2%BA%203.214%20(aprova%20as%20NRs).pdf)

Brasil (2010) Lei Federal n. 12.305 de 02 de agosto de 2010. Dispõe sobre a Política Nacional de Resíduos Sólidos; [accessed 2015 February 25]. [http://www.planalto.gov.br/ccivil\\_03/\\_ato2007-2010/2010/lei/l12305.htm](http://www.planalto.gov.br/ccivil_03/_ato2007-2010/2010/lei/l12305.htm)

Delhaès P, Trinquécoste M, Derré A, Rovillain D, David P (2003) Film boiling chemical vapor infiltration of C/C composites: influence of mass and thermal transfers. *Carbon Science* 4(4):163-167.

Delhaès P, Trinquécoste M, Lines J-F, Cosculluela A, Goyhénèche J-M, Couzi M (2005) Chemical vapor infiltration of C/C composites: fast densification processes and matrix characterization. *Carbon* 43(4):681-691. doi: 10.1016/j.carbon.2004.10.030

Houdayer M, Spitz J, Tran-Van D, inventors (1984) Process for the densification of a porous structure. United States patent US 4472454.

Li W, Zhang SY, Yan XF, Li HJ, Li KZ (2010) Densification and microstructure of carbon/carbon composites prepared by chemical vapor infiltration using ethanol as precursor. *Sci China Tech Sci* 53(8):2232-2238. doi: 10.1007/s11431-009-3161-y

Maslova OA, Ammar MR, Guimbretière G, Rouzaud J-N, Simon P (2012) Determination of crystallite size in polished graphitized carbon by Raman spectroscopy. *Phys Rev B* 86(13):134205. doi: 10.1103/PhysRevB.86.134205

Murdie N (1993) Carbon-Carbon Matriz Materials. In: Buckley JD, Edie DD. *Carbon-carbon materials and composites*. New Jersey: Noyes Publications. p. 105-168.

Nadeau N, Vignoles GL, Brauner C-M (2006) Analytical and numerical study of the densification of carbon/carbon composites by a film-boiling chemical vapor infiltration process. *Chemical Engineering Science* 61(22):7509-7527. doi: 10.1016/j.ces.2006.08.027

Rovillain D, Trinquécoste M, Bruneton E, Derré A, David P, Delhaès P (2001) Film boiling chemical vapor infiltration: an experimental study on carbon/carbon composite materials. *Carbon* 39(9):1355-1365. doi: 10.1016/S0008-6223(00)00255-4

Savage G (1993) *Carbon-carbon composites*. London: Chapman & Hall. Chapter 1, Introduction; p. 1-36.

Vignoles GL, Ducloux R, Gaillard S (2007) Analytical stability study of the densification front in carbon- or ceramic-matrix composites processing by TG-CVI. *Chemical Engineering Science* 62(22):6081-6089. doi: 10.1016/j.ces.2007.06.022

Vignoles GL, Goyhénèche J-M, Sébastien P, Puiggali J-R, Lines J-F, Lachaud J, Delhaès P, Trinquécoste M (2006) The film-boiling densification process for C/C composite fabrication: from local scale to overall optimization. *Chemical Engineering Science* 61(17):5636-5653. doi: 10.1016/j.ces.2006.04.025

Vignoles GL, Nadeau N, Brauner C-M, Lines J-F, Puiggali J-R (2005) The notion of densification front in CVI processing with temperature gradients. In: Lara-Curzio E, editor. *Ceramic Engineering and Science Proceedings*. Oxford: John Wiley and Sons, The American Ceramics Society. p. 187-185. doi: 10.1002/9780470291221.ch23

Wang J, Qian J, Qiao G, Jin Z (2007) A rapid fabrication of C/C composites by a thermal gradient chemical vapor infiltration method with vaporized kerosene as a precursor. *Materials Chemistry and Physics* 101(1):7-11. doi: 10.1016/j.matchemphys.2006.02.006